Available online at www.sciencedirect.com
ScienceDirect
Solar Energy 81 (2007) 1482–1491
SOLAR ENERGY
www.elsevier.com/locate/solener

The influence of binary mixture thermophysical properties in the analysis of heat and mass transfer processes in solar distillation systems

P.T. Tsilingiris [1]

Department of Energy Engineering, Technological Education Institution (TEI) of Athens, A.Spyridonos str. GR 122 10, Egaleo, Athens, Greece

Received 7 August 2006; received in revised form 9 February 2007; accepted 16 February 2007
Available online 15 March 2007

Communicated by: Associate Editor G.N. Tiwari

Abstract

Although a substantial amount of research work has already been devoted to various aspects of modeling the convective and mass transport processes in solar distillation systems, it appears that the role of thermophysical and transport properties of the working medium and their effect on the thermal behavior and performance analysis of such systems has been left almost completely unnoticed. The working medium in these systems, which is a binary mixture of water vapor and dry air in equilibrium, appears to exhibit a completely different set of properties than dry air, especially at saturation conditions and at the higher region of the solar still operational temperature range. An analysis is presented aiming to signify the effect of binary mixture thermophysical properties on the transport processes and the associated quantities and evaluate the thermophysical properties of the working medium in these systems, based on contemporary data for dry air and water vapor. The derived results, in the form of convenient algebraic correlations, are employed to investigate the effect of using the appropriate thermophysical properties on the calculation of the convective heat and mass transfer, as well as the distillate mass flow rates. According to the results from the present investigation, although the use of improper dry air data leads to a significant overestimation of the convective heat transfer coefficient, the errors associated with the use of improper dry air properties is a moderate overestimation of distillate output which is estimated to be up to 10% for maximum average still temperatures of 100 °C.

Keywords: Solar distillation; Heat and mass transfer analysis; Binary mixture properties; Thermophysical properties of saturated air

1. Introduction

Owing to the limited freshwater resources in certain geographical regions of the world the technological and economic prospects of solar desalination, which is an energy intensive process, appears to be very promising to supply fresh water at higher than the survival level quantities in a wide range of latitudes around the equator zones. At these locations, where land is free, solar energy is abundant and in-phase with the peak water demand, the solar distillation appears to offer an environmentally friendly and economically viable option. Although the original idea is very old, the scientific research and the systematic investigation of the pertinent physical processes occurring in these systems began only about five decades ago. This research has led to the development of simple solar stills of mature design and appropriate technology level for applications in developing countries and isolated offshore communities. Several remarkable full scale pilot and commercial plants were operated worldwide (Lof, 1980) until the ceasing of research activities, almost forty years ago. The revived interest over the last few decades, is mainly attributed to the escalation of energy cost and the serious environmental concerns in the present day society. This has led to various substantial improvements in design and performance (Fath

E-mail address: ptsiling@teiath.gr
[1] ISES Member.

0038-092X/$ - see front matter © 2007 Elsevier Ltd. All rights reserved.
doi:10.1016/j.solener.2007.02.005

Nomenclature

$A_0, A_1, \ldots, A_4$ numerical constants
c_p specific heat capacity (J/kg °K)
C numerical constant
$CA_0, CA_1, \ldots, CA_4$ numerical constants
$CP_0, CP_1, \ldots, CP_4$ numerical constants
CV_0, CV_1, CV_2 numerical constants
$g = 9.81$ m/s^2 acceleration of gravity
h heat transfer (W/m^2 °K) or mass transfer (m/s) coefficient
h_{fg} heat of evaporation (kJ/kg)
HF_0, HF_1 numerical constants
Gr Grashof number (−)
k thermal conductivity (W/m °K)
$K_0, K_1, \ldots, K_3$ numerical constants
$KA_0, KA_1, \ldots, KA_5$ numerical constants
KV_0, KV_1, KV_2 numerical constants
L characteristic length (m)
M molecular weight (kg/kmol)
$\dot{m}$ mass flow rate (kg/m^2 s)
$MA_0, MA_1, \ldots, MA_4$ numerical constants
MV_0, MV_1 numerical constants
$MU_0, MU_1, \ldots, MU_4$ numerical constants
n numerical exponent
N number of molecules
P pressure (Pa)
Pr Prandtl number (−)
q heat flux (W/m^2)
R gas constant (kJ/kg °K)
$\overline{R}$ universal gas constant (kJ/kmol °K)
Ra Rayleigh number (−)
RH relative humidity
$RO_0, RO_1, \ldots, RO_3$ numerical constants
t temperature (°C)
T absolute temperature (°K)
T^* equivalent temperature (°K)
$TD_0, TD_1, \ldots, TD_4$ numerical constants
x molar fraction (−)
w specific humidity (kg water vapor/kg dry air)
z compressibility factor

Greek letters
α thermal diffusivity (m^2/s)
β volumetric expansion coefficient (K^{-1})
ΔT temperature difference (°C)
ΔT^* equivalent temperature difference (°C)
μ viscosity (N s/m^2)
ν kinematic viscosity (m^2/s)
ρ density (kg/m^3)

Subscripts
a air
ag air at condensing surface
as air at liquid surface
cv convective
e evaporative
g condensing surface
m mixture
o total
s liquid interface
sv saturated vapor
v vapor
vg water vapor at the condensing surface
vs water vapor at the liquid surface
w distillate

and Elsherbiny, 1992; Rahim and Taqi, 1992; Tiwari et al., 1993; Haddat et al., 2000; Aggrawal and Tiwari, 1998; Ahmed, 1988), although sometimes of a questionable worth, owing to the corresponding sacrifice of system simplicity and long-term reliability which are serious advantages deserving the key role for dissemination in a low technology environment. The evolution of powerful computing facilities has allowed a much deeper insight on the parameters, influencing the dynamic behavior of simple and more complex systems (Cooper, 1969; Al Mahdi, 1992), beyond the level of the first analytical model presented by Duncle (1961). This model was developed under certain stringent limitations and its predictive accuracy appears sometimes to be rather poor, leading to conflicting results with experimental measurements (Kumar and Tiwari, 1996; Clark, 1990). This is attributed to the several complex, interrelated, design sensitive and temperature dependent processes, concurring simultaneously in a so simple engineering system.

The application of this model which was extensively employed for performance predictions and comparative analyses (Malik et al., 1982), is based on the use of thermophysical properties of the working medium, which is a saturated binary mixture of dry atmospheric air and water vapor. Dry atmospheric air, seen as a multi component system of various gases, has a different molecular weight, gas constant and thermophysical properties, than water vapor. Therefore, the thermophysical properties of humid air are strong functions of humidity ratio and mixture temperature. Reports on such properties are few and relevant data which have sporadically appeared in the literature to cover mostly specific metrological or calibration applications (Wong and Embleton, 1984; Zuckerwar and Meredith, 1985; Giacomo, 1982; Melling et al., 1997), are incomplete for the purpose of solar distillation system analyses, covering a completely different temperature range than the range of interest in solar stills. Owing to the lack of suitable data and for the purpose of first order calculations, especially at

lower temperatures when the mixture is far from saturation conditions, one can replace the thermophysical properties of moist air by those corresponding to dry air, without a significant sacrifice of accuracy. For this reason, average dry air or even better temperature dependent dry air thermophysical properties may be employed. However, this is not acceptable for improved accuracy calculations, especially at higher temperatures when the mixture is close to saturation, as it is usually the case during the operation of solar stills. To the author's knowledge, apart from very limited, scarce and incomplete reports in the literature, a complete account of thermophysical properties for the humid air at the temperature range of interest in solar stills is lacking from the literature. It appears as though that a substantial part of the earlier and more recent investigations (Tiwari et al., 1997; Aggrawal and Tiwari, 1998), has been based on data available from few, repeatedly appearing literature sources as in Al Mahdi (1992) from Wong and Embleton (1984) and Toyama et al. (1987), which were supposed to offer thermophysical properties for humid air. However, a careful inspection of these data and comparison with corresponding dry air data from standard contemporary literature sources (Irvine, 1998), indicates that they essentially correspond to dry air. This is shown in Fig. 1 in which the three main transport properties involved in the heat and mass transfer analyses, namely viscosity, thermal conductivity and specific heat capacity were plotted for comparison in the typical temperature range of interest. In this plot data from Al Mahdi (1992) (broken lines), and Toyama et al. (1987) (thin solid lines) which are repeatedly appearing in the literature as humid air properties are compared to dry air properties from and Irvine (1998) (heavy solid lines). Although insignificant differences in the order of 2% are observed for viscosity, the thermal conductivity and specific heat capacity from these literature sources are almost identical to the properties of dry air, clearly confirming that they refer to dry air.

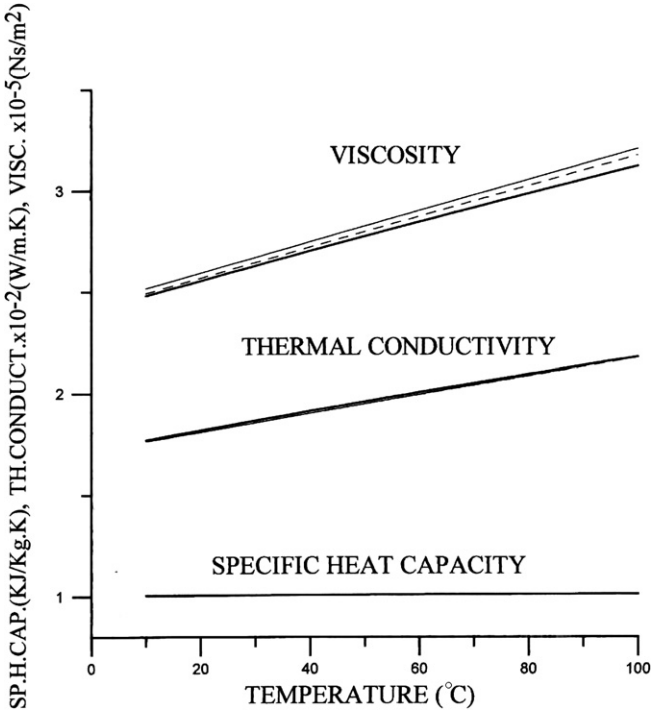

Fig. 1. Comparative presentation of specific heat capacity, thermal conductivity and viscosity data from Al Mahdi (1992) (broken lines), Toyama et al. (1987) (thin solid lines) with Irvine (1998) (heavy solid lines) for dry atmospheric air, in the temperature range between 10 and 100 °C.

The aim of the present work is the description of simple procedures for the first order evaluation of the thermophysical properties of humid air, based on dry air and water vapor properties. The derived data are employed for the investigation of the effects and implications of using improper thermophysical data, other than those corresponding to saturated humid air, on the accuracy of the analytical description and heat and mass transfer calculations leading to the theoretical prediction of convective and evaporative heat transfer, as well as on the distillate productivity in solar distillation systems. Towards this aim an analysis of the heat and mass transfer processes is presented, aiming to identify the description of the crucial operational parameters influencing the system performance which are affected by the transport properties of the saturated binary mixture.

2. Combined heat and mass transfer processes in solar stills

While natural convection heat transfer, induced by the temperature differential Δt between two fluid regions is determined by the value of the ordinary Grashof number,

$$Gr = \frac{g\beta L^3 \Delta t}{\nu^2} \tag{1}$$

the mass transfer is taking place owing to a fluid density differential, which is a function of temperature and composition. Since the water vapor is lighter than dry air, the evaporation actually increases the driving buoyancy force, represented by Δt in (1), which leads to the definition of the modified Grashof number according to Coulson and Richardson (1961) is,

$$Gr^* = \frac{gL^3}{\nu_m^2}\left(\frac{\rho_{m,g}}{\rho_{m,s}} - 1\right) \tag{2}$$

where $\rho_{m,s}$ and $\rho_{m,g}$ the mixture density at the two fluid regions. The above expression can be applied in the space between the free liquid surface and the top condensing plate of a solar still, at temperatures T_s and T_g, respectively. Assuming that the working fluid in the still is a binary mixture of two gaseous components in equilibrium, namely dry air and water vapor respectively, the molecular weights of the mixture at the brine and condensing surface, $M_{m,s}$ and $M_{m,g}$, respectively, are not equal. Applying the gas law, which is assumed to be valid at the two regions in the binary mixture, the previous expression becomes,

$$Gr^* = \frac{g\rho_m^2 L^3}{\mu_m^2}\left(\frac{M_{m,g}T_s}{M_{m,s}T_g} - 1\right) \tag{3}$$

However the molecular weight of mixture at the two fluid regions is a function of the molar fractions x_{vs}, x_{as} and the molecular weights M_v, M_a of water vapor and dry air of each component, respectively,

$$M_{m,s} = M_v x_{vs} + M_a x_{as} \tag{4}$$

with,

$$x_{vs} = \frac{N_{vs}}{N_{vs}+N_{as}} = \frac{P_{vs}}{P_o} \tag{5}$$

$$x_{as} = \frac{N_{as}}{N_{vs}+N_{as}} = \frac{P_{as}}{P_o} \tag{6}$$

where, N_{vs}, N_{as}, P_{vs} and P_{as} are the number of water and air moles and the respective partial water vapor and dry air pressure at the water–air interface. It is derived from (4)–(6) that,

$$M_{m,s} = M_v \frac{P_{vs}}{P_o} + M_a \frac{P_{as}}{P_o} \tag{7}$$

In a similar way it is derived that the molar mass of humid air at the condensing surface is expressed as,

$$M_{m,g} = M_v \frac{P_{vg}}{P_o} + M_a \frac{P_{ag}}{P_o} \tag{8}$$

with P_{vg}, P_{ag} the partial water vapor and dry air pressures at the condensing surface. The quantity $\left(\frac{M_{m,g}T_s}{M_{m,s}T_g} - 1\right)$ in the expression (3) can be calculated using the values of $M_{m,s}$ and $M_{m,g}$ from (7) and (8), taking into account that,

$$P_{vs} + P_{as} = P_{vg} + P_{ag} = P_o \tag{9}$$

where P_o the atmospheric pressure. Assuming that $\beta \approx T_g^{-1}$, after algebraic manipulations it is finally derived that,

$$\frac{M_{m,g}T_s}{M_{m,s}T_g} - 1 = \beta\left[\Delta t + \frac{(P_{vg}-P_{vs})(M_v-M_a)T_s}{M_a P_o + P_{vs}(M_v-M_a)}\right] \tag{10}$$

where $\Delta t = t_s - t_g$. Taking into account (10), the expression (3) written for the values of thermophysical properties corresponding to the binary mixture of saturated vapor and dry air yields,

$$Gr^* = \frac{g\rho_m^2 L^3}{\mu_m^2}\beta\left[\Delta t + \frac{(P_{vg}-P_{vs})(M_v-M_a)T_s}{M_a P_o + P_{vs}(M_v-M_a)}\right] \tag{11}$$

Since by definition $Ra = GrPr$, the modified dimensionless Rayleigh number for the binary mixture is defined as,

$$Ra^* = \frac{g\rho_m \beta L^3 \Delta T^*}{\mu_m \alpha_m} \tag{12}$$

where, the equivalent temperature difference

$$\Delta T^* = (T_s - T_g) + T_s \frac{(P_{vs}-P_{vg})(M_a-M_v)}{M_a P_o - P_{vs}(M_a-M_v)} \tag{13}$$

is higher than the temperature difference $\Delta T = T_s - T_g$. For an enclosed horizontal space the relationship between Nusselt and Grashof number is described by,

$$Nu = C\,Ra^n \tag{14}$$

where C and n are numerical constants depending on boundary conditions and the flow regime. The evaluation of these constants has been the objective of various earlier and more recent investigations, based on dry air. For example McAdams (1981) suggested $C = 0.21$, $n = 0.25$ for Grashof numbers from 10^4 to 3.2×10^5, and $C = 0.075$, $n = 0.333$ for Grashof numbers from 3.2×10^5 to 10^7, while Hollands et al. (1975) suggests that for $Ra > 5\times10^6$ the corresponding constants are $C = 0.0555$, $n = 0.333$. Duncle (1961) has suggested that for humid air enclosed in a horizontal space, the numerical constants in (14) are $C = 0.075$, $n = 0.333$ for $3.2\times10^5 < Gr < 10^7$.

Combining the expressions (12)–(14), it is derived that,

$$h_{cv} = C k_m \left(\frac{g\rho_m\beta}{\mu_m\alpha_m}\right)^{1/3}\left[(T_s - T_g) + \frac{T_s(P_{vs}-P_{vg})(M_a-M_v)}{M_a P_o - P_{vs}(M_a-M_v)}\right]^{1/3} \tag{15}$$

where k_m, ρ_m, μ_m and α_m the thermophysical properties of the saturated mixture. The upwards heat flux in the still represents the sum of the sensible heat transfer owing to the convective circulation of dry air within the solar still enclosure and the latent heat transfer owing to the direct transport of water vapor from the liquid surface, where the water evaporates at the temperature T_s, to the top surface where it condenses as distillate at the temperature T_g. Having previously determined the natural convective heat transfer coefficient in the solar still enclosure through the expression (15), the sensible heat transfer per unit still area is,

$$q_{cv} = h_{cv}(T_s - T_g) \tag{16}$$

However, since this quantity involves the convective circulation of dry air it can also be expressed in terms of the corresponding mass flow rate and specific heat capacity of dry air by the following expression,

$$q_{cv} = \dot{m}_a c_{pa}(T_s - T_g) \tag{17}$$

where $\dot{m}_a$ and c_{pa} the mass flow rate per unit area of the still and the specific heat capacity of dry air, respectively.

It is derived from (16) and (17) that,

$$\dot{m}_a = \frac{h_{cv}}{c_{pa}} \tag{18}$$

The specific humidity of the mixture at the pool surface is defined as the mass of water vapor to the mass of dry air at the surface,

$$w_s = \frac{m_{vs}}{m_{as}} \tag{19}$$

Assuming ideal gas behavior of both components, it is easily derived from the previous expression that,

$$w_s = \frac{P_{vs}}{P_{as}}\frac{R_a}{R_v} = \frac{P_{vs}}{P_o - P_{vs}}\frac{R_a}{R_v} \tag{20}$$

The mass of water vapor transferred from the pool surface is,

$$\dot{m}_a w_s = \frac{h_{cv}}{c_{pa}}\frac{P_{vs}}{P_o - P_{vs}}\frac{R_a}{R_v} \tag{21}$$

The specific humidity of the mixture at the top condensing surface temperature is derived by an expression which is similar to (20),

$$w_g = \frac{P_{vg}}{P_{ag}}\frac{R_a}{R_v} = \frac{P_{vg}}{P_o - P_{vg}}\frac{R_a}{R_v} \tag{22}$$

The mass of distillate per unit area and time (kg/m^2 s) transferred at the top condensing surface is,

$$\dot{m}_a w_g = \frac{h_{cv}}{c_{pa}}\frac{P_{vg}}{P_o - P_{vg}}\frac{R_a}{R_v} \tag{23}$$

The mass flow rate of distillate at the top condensing surface is derived by the difference of the left hand side quantities in expressions (21) and (23)

$$\dot{m}_a(w_s - w_g) = \frac{h_{cv}}{c_{pa}}\frac{R_a}{R_v}\left(\frac{P_{vs}}{P_o - P_{vs}} - \frac{P_{vg}}{P_o - P_{vg}}\right) \tag{24}$$

The rejected energy at the top condensing surface owing to the condensation of the water vapor is the product of water mass transfer times the latent heat of water vaporization at the specific temperature,

$$q_{ev} = 1000 h_{fg}\dot{m}_a(w_s - w_g) \tag{25}$$

with the numerical multiplier 1000 introduced to account the units of the quantity h_{fg}, usually expressed in kJ/kg, as indicated in the nomenclature. Therefore from (24) and (25) it is derived that,

$$q_{ev} = 1000 h_{fg}\frac{h_{cv}}{c_{pa}}\frac{R_a}{R_v}\cdot\left(\frac{P_{vs}}{P_o - P_{vs}} - \frac{P_{vg}}{P_o - P_{vg}}\right) \tag{26}$$

However, since,

$$q_{ev} = h_e(P_{vs} - P_{vg}) \tag{27}$$

the evaporative heat transfer coefficient (m/s) is calculated from (26) and (27) as,

$$h_e = 1000 h_{fg}\frac{h_{cv}}{c_{pa}}\frac{R_a}{R_v}\frac{P_o}{(P_o - P_{vs})(P_o - P_{vg})} \tag{28}$$

The condensed water mass per unit still area and time is calculated by,

$$\dot{m}_w = \frac{q_{ev}}{1000 h_{fg}} \tag{29}$$

which, taking into account the expression (26) becomes,

$$\dot{m}_w = \frac{h_{cv}}{c_{pa}}\frac{R_a}{R_v}\left[\frac{P_o(P_{vs} - P_{vg})}{(P_o - P_{vs})(P_o - P_{vg})}\right] \tag{30}$$

3. The evaluation of thermophysical and transport properties of humid air

For the purpose of determining the thermophysical and transport properties of the humid air, the dry atmospheric air is regarded as a pseudo-pure component of a standard composition as typically given by Giacomo (1982). The molar fraction of water vapor x_v as defined by the expression (5) is the ratio of the partial water vapor to the total pressure. According to Melling et al. (1997), simple mixing correlations for both components of the binary mixture, the pure water vapor and dry air at the partial pressures and molar fractions P_v, x_v and $P_a = P_o - P_v$, $x_a = 1 - x_v$, respectively, are offering sufficient accuracy for derivation of results, suitable for ordinary engineering heat transfer calculations.

3.1. Density

Assuming that both components under the atmospheric pressure are behaving as ideal gases, the density of mixture is calculated by,

$$\rho_m = \frac{1}{z}\frac{P_o}{\overline{R}T}\left(M_a\frac{P_o - P_v}{P_o} + M_v\frac{P_v}{P_o}\right) \tag{31}$$

In the above expression the universal gas constant is $\overline{R} = 8.314$ kJ/kmol °K and the compressibility factor z was taken to be close to unity for the conditions under consideration. Assuming that the relative humidity of the mixture is defined as,

$$\mathrm{RH} = \frac{P_v}{P_{sv}} \tag{32}$$

the expression (31) becomes,

$$\rho_m = \frac{P_o}{\overline{R}T}\left[M_a\left(1 - \mathrm{RH}\frac{P_{sv}}{P_o}\right) + M_v\mathrm{RH}\frac{P_{sv}}{P_o}\right] \tag{33}$$

where, P_{sv} the partial pressure of saturated vapor. Although P_{sv} can readily be available through several classical correlations in the literature (Alduchov and Escridge, 1997), they are not valid for the entire temperature range of interest. Therefore for the purpose, the following correlation was derived by fitting of numerical values of saturation vapor pressure in (kPa) between 10 and 110 °C, available from the thermodynamic properties of water (steam tables) (Van Wilen and Sonntag, 1973),

$$P_{sv} = A_0 + A_1 t + A_2 t^2 + A_3 t^3 + A_4 t^4 \tag{34}$$

with the numerical values of constants $A_0 = 1.131439334$, $A_1 = -3.750393331 \times 10^{-2}$, $A_2 = 5.591559189 \times 10^{-3}$, $A_3 = -6.220459433 \times 10^{-5}$, $A_4 = 1.10581611 \times 10^{-6}$.

The derived mixture density is shown in Fig. 2, in which it is plotted against temperature, with the relative humidity varying from RH = 0% corresponding to dry air (top line) to a saturated mixture at RH = 100% (bottom line) as a parameter. A comparative inspection between lines suggests that mixture density at a constant temperature decreases significantly as the molar fraction of water vapor increases, and the saturated mixture density is appreciably lower than dry air density, especially at higher temperatures. The results corresponding to saturated humid air mixture density in (kg/m^3) were fitted by the following third order polynomial function,

$$\rho_m = \mathrm{RO}_0 + \mathrm{RO}_1 t + \mathrm{RO}_2 t^2 + \mathrm{RO}_3 t^3 \tag{35}$$

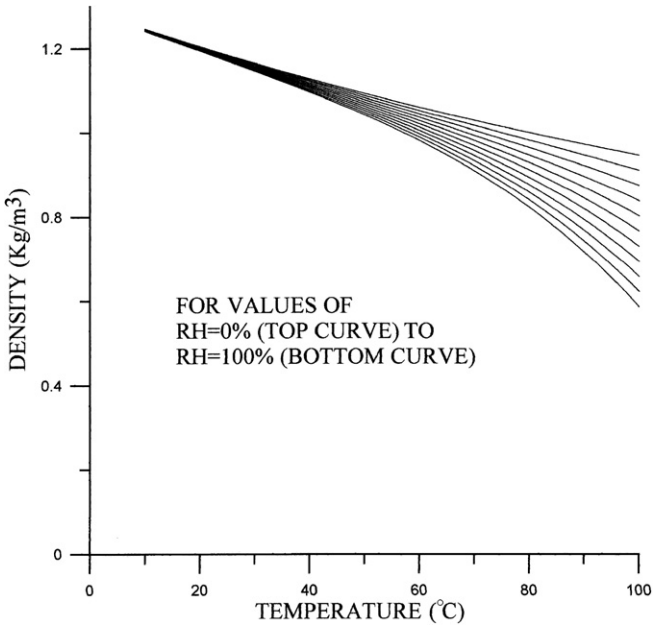

Fig. 2. The density of a water vapor and dry air mixture with a relative humidity ranging between RH = 0% (top line) corresponding to dry air and a saturated mixture of RH = 100% (lower line), with all the intermediate curves corresponding to an increasing relative humidity step of 10%, as a function of temperature between 10 and 100 °C.

with the values of numerical constants, $RO_0 = 1.299995662$, $RO_1 = -6.043625845 \times 10^{-3}$, $RO_2 = 4.697926602 \times 10^{-5}$, $RO_3 = -5.760867827 \times 10^{-7}$, with a coefficient of determination of 0.999975.

3.2. Viscosity

For the evaluation of viscosity according to linear mixing considerations, the Krischer and Kast (1978) correlation was employed as recommended in Melling et al. (1997),

$$\mu_m = \frac{\mu_a(P_o - P_v)\sqrt{M_a} + \mu_v P_v \sqrt{M_v}}{(P_o - P_v)\sqrt{M_a} + P_v\sqrt{M_v}} \tag{36}$$

The viscosity of dry air μ_a in ($N\,s/m^2 \times 10^{-6}$), was taken for the temperature range of $-23\,°C \leqslant t \leqslant 327\,°C$,

by the following correlation,

$$\mu_a = MA_0 + MA_1 T + MA_2 T^2 + MA_3 T^3 + MA_4 T^4 \tag{37}$$

in $Ns/m^2 \times 10^{-6}$ from Irvine (1998) as compiled from Irvine and Liley (1984), with $MA_0 = -9.8601 \times 10^{-1}$, $MA_1 = 9.080125 \times 10^{-2}$, $MA_2 = -1.17635575 \times 10^{-4}$, $MA_3 = 1.2349703 \times 10^{-7}$, $MA_4 = -5.7971299 \times 10^{-11}$.

The viscosity values of water vapor in ($N\,s/m^2 \times 10^{-7}$) at the temperature range $0 \leqslant t \leqslant 120\,°C$, were derived by the following linear expression,

$$\mu_v = MV_0 + MV_1 t \tag{38}$$

with $MV_0 = 80.58131868$ and $MV_1 = 0.4000549451$ as reported in Irvine (1998) and compiled from Toulukian et al. (1970).

Derived results of mixture viscosity are shown in the Fig. 3, for a relative humidity ranging between 0% and RH = 100%. According to these, the effect of water vapor content increase up to the saturation level being relatively small, almost to only 3% for the temperatures up to 40 °C, it becomes quite significant at saturation conditions and temperatures up to 100 °C. For saturated conditions the viscosity increases up to its maximum value at around 50 °C, before it rapidly declines at higher temperatures.

The derived results for the viscosity of the saturated humid air in ($N\,s/m^2$) were fitted by the following fourth order polynomial function,

$$\mu_m = MU_0 + MU_1 t + MU_2 t^2 + MU_3 t^3 + MU_4 t^4 \tag{39}$$

with the values of numerical constants, $MU_0 = 1.685731754 \times 10^{-5}$, $MU_1 = 9.151853945 \times 10^{-8}$, $MU_2 = -2.16276222 \times 10^{-9}$, $MU_3 = 3.413922553 \times 10^{-11}$, $MU_4 = -2.644372665 \times 10^{-13}$ and with a coefficient of determination of 0.999843.

3.3. Specific heat capacity

The specific heat capacity of moist air can be derived by the following expression,

$$c_{pm} = c_{pa}(1 - x_v)\frac{M_a}{M_m} + c_{pv}x_v\frac{M_v}{M_m} \tag{40}$$

where, M is the molar mass of humid air, which is calculated by,

$$M_m = M_a(1 - x_v) + M_v x_v \tag{41}$$

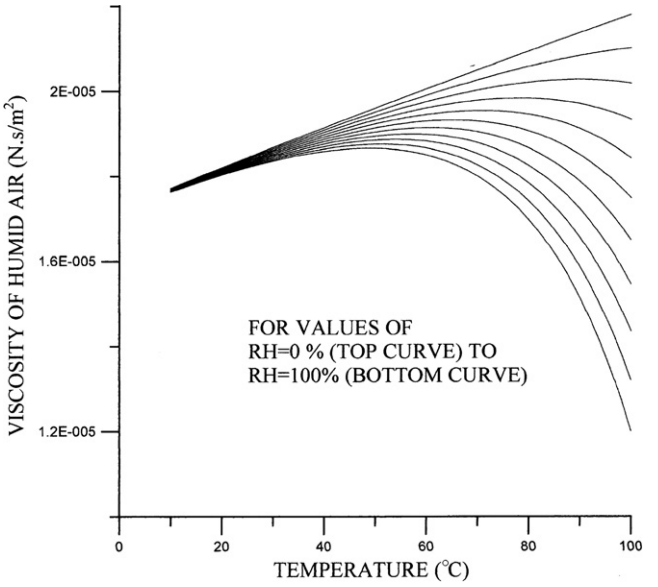

Fig. 3. Viscosity of a water vapor and dry air mixture of a relative humidity ranging between RH = 0% (top line) and a saturated mixture of RH = 100% (lower line), with all the intermediate curves corresponding to an increasing relative humidity step of 10%, as a function of temperature between 10 and 100 °C.

Combining (40) and (41) it is derived that,

$$c_{pm} = \frac{c_{pa}(P_o - P_v)M_a + c_{pv}P_vM_w}{M_a(P_o - P_v) + M_vP_v} \quad (42)$$

Data for dry air specific heat capacity in (kJ/kg K) were derived from Irvine (1998) as compiled from Irvine and Liley (1984), which are given from the following expression,

$$c_{pa} = CA_0 + CA_1T + CA_2T^2 + CA_3T^3 + CA_4T^4 \quad (43)$$

valid for the same temperature range $250 < T < 1050$ K, with values of $CA_0 = 1.03409$, $CA_1 = -0.284887 \times 10^{-3}$, $CA_2 = 0.7816818 \times 10^{-6}$, $CA_3 = -0.4970786 \times 10^{-9}$ and $CA_4 = 0.1077024 \times 10^{-12}$.

Water vapor specific heat capacity data in (kJ/kg K) were derived from Toulukian et al. (1970) by the following expression,

$$c_{pv} = CV_0 + CV_1t + CV_2t^2 \quad (44)$$

which is valid for the temperature range $0 < t < 120$ °C, with values of $CV_0 = 1.86910989$, $CV_1 = -2.578421578 \times 10^{-4}$ and $CV_2 = 1.941058941 \times 10^{-5}$.

Derived results are shown in Fig. 4, in which the specific heat capacity of mixture is plotted against temperature, with the relative humidity as a parameter ranging between 0% and RH = 100%. It can be seen that while for the low temperature range up to 40 °C the effect of moisture is relatively small, leading to a specific heat capacity increase of up to 4.5%, it becomes quite significant at temperatures close to 100 °C and saturation conditions.

The derived results for the saturated mixture in (kJ/kg K) were fitted by the following fourth order polynomial,

$$c_{pm} = CP_0 + CP_1t + CP_2t^2 + CP_3t^3 + CP_4t^4 \quad (45)$$

with the values of numerical constants, $CP_0 = 1.088022802$, $CP_1 = -0.01057758092$, $CP_2 = 4.769110559 \times 10^{-4}$, $CP_3 = -7.898561559 \times 10^{-6}$, $CP_4 = 5.122303796 \times 10^{-8}$ and with a coefficient of determination of 0.999458.

3.4. Thermal conductivity

As derived from simple mixing considerations the thermal conductivity of moist air is given by the following expression,

$$k_m = k_a(1 - x_v) + k_vx_v \quad (46)$$

Values of thermal conductivity of dry air and water vapor were derived from Irvine (1998) by the following correlations,

$$k_a = KA_0 + KA_1T + KA_2T^2 + KA_3T^3 + KA_4T^4 + KA_5T^5 \quad (47)$$

for dry air in (W/m K), for the temperature range between $250 < T < 1050$ K, with $KA_0 = -2.276501 \times 10^{-3}$, $KA_1 = 1.2598485 \times 10^{-4}$, $KA_2 = -1.4815235 \times 10^{-7}$, $KA_3 = 1.73550646 \times 10^{-10}$, $KA_4 = -1.066657 \times 10^{-13}$, $KA_5 = 2.47663035 \times 10^{-17}$ and

$$k_v = KV_0 + KV_1T + KV_2T^2 \quad (48)$$

for water vapor in (W/m K $\times 10^{-3}$), at the temperature range of $0 < T < 120$ °C with, $KV_0 = 17.61758242$, $KV_1 = 0.05558941059$ and $KV_2 = 0.0001663336663$.

The derived results were plotted in Fig. 5 as a function of temperature for the relative humidity ranging from 0 (top line) to RH = 100% (lower curve) as a parameter,

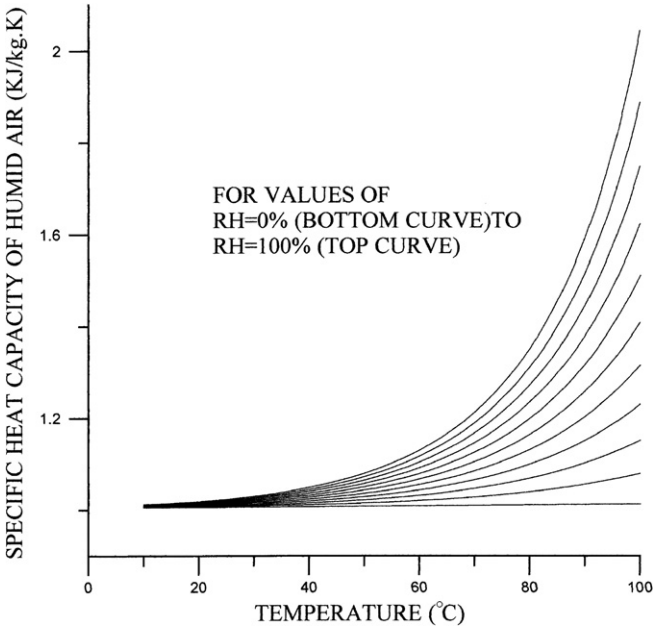

Fig. 4. Specific heat capacity of a water vapor and dry air mixture of a relative humility ranging between RH = 0% (bottom line) and a saturated mixture of RH = 100% (top line), with all the intermediate curves corresponding to an increasing relative humidity step of 10%, as a function of temperature between 10 and 100 °C.

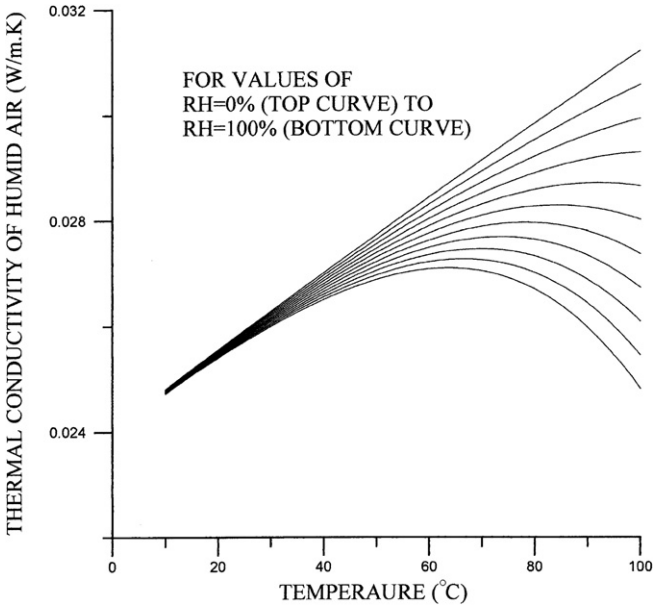

Fig. 5. Thermal conductivity of a water vapor and dry air mixture of a relative humidity ranging between RH = 0% (top line) and a saturated mixture of RH = 100% (lower line), with all the intermediate curves corresponding to an increasing relative humidity step of 10%, as a function of temperature between 10 and 100 °C.

showing a significant effect of moisture content on the thermal conductivity of the mixture. Although for a constant relative humidity lower than about 40% it increases monotonically with temperature, for RH > 40% it becomes maximum at a temperature which decreases as the relative humidity increases up to saturation conditions. Although the effect of saturation at low temperatures up to 40 °C leads to an insignificant, almost about 2% decrease of dry air thermal conductivity, its effect is remarkable at higher temperatures, leading to remarkable, almost 80% decrease of thermal conductivity at temperatures up to 100 °C. Appropriate fitting of the calculated data leads to the following polynomial expression for the thermal conductivity of the saturated mixture in (W/m K),

$$k_m = K_0 + K_1 t + K_2 t^2 + K_3 t^3 \quad (49)$$

with $K_0 = 0.02416826077$, $K_1 = 5.526004579 \times 10^{-5}$, $K_2 = 4.631207189 \times 10^{-7}$, $K_3 = -9.489325324 \times 10^{-9}$, which is valid in the temperature range between 10 and 100 °C with a coefficient of determination equal to 0.999737.

3.5. Thermal diffusivity

It is calculated from its definition expression,

$$a_m = \frac{k_m}{\rho_m c_m} \quad (50)$$

taking into account the previously derived thermophysical property correlations (35), (45) and (49) for a saturated mixture. The results are plotted in the Fig. 6, in which the significant effect of moisture content on the mixture thermal diffusivity is shown, which is responsible for up to about 60% thermal diffusivity reduction for saturated mixture temperatures up to 100 °C.

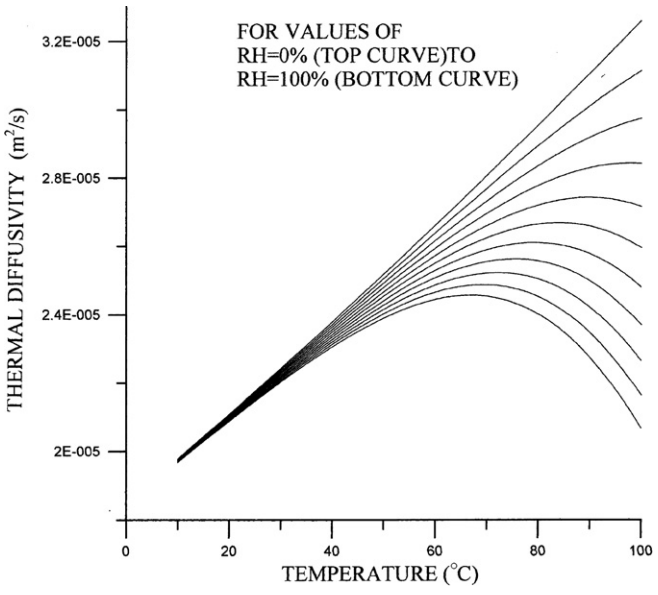

Fig. 6. Thermal diffusivity of a water vapor and dry air mixture with a relative humidity ranging between RH = 0% (top line) and a saturated mixture of RH = 100% (lower line), with all the intermediate curves corresponding to an increasing relative humidity step of 10%, as a function of temperature between 10 and 100 °C.

The derived results for a saturated air mixture in (m^2/s) at the temperature range of interest, were fitted by the following fourth order polynomial expression,

$$\alpha_m = TD_0 + TD_1 t + TD_2 t^2 + TD_3 t^3 \quad (51)$$

with, $TD_0 = 1.881493006 \times 10^{-5}$, $TD_1 = 8.027692454 \times 10^{-8}$, $TD_2 = 1.496456991 \times 10^{-9}$, $TD_3 = -2.112432387 \times 10^{-11}$ and with a coefficient of determination of 0.999744.

4. The comparative influence of saturated mixture properties

The investigation of the comparative influence of mixture thermophysical properties is possible by plotting the predicted values of convective heat transfer coefficient from (15) as a function of the average still temperature, with the temperature difference between brine and condensing plate as a parameter. Although the numerical value of the constant C depends on several design and operational parameters of the still, for the purpose of the present investigation it was fixed to $C = 0.075$. The working medium is assumed to be a saturated binary mixture of dry atmospheric air and water vapor, something which represents more or less typically the conditions in solar still practice, with a thermal conductivity, density, viscosity and thermal diffusivity of mixture derived from the correlations (49), (35), (39) and (51), respectively. The saturated vapor pressure at the temperature range of interest is given by the expression (34), with molecular weights for dry air and water vapor 28.97 and 18.02 kg/kmol, respectively, and a standard atmospheric pressure of $P_o = 101.3$ kPa. Calculation of the relevant results were also alternatively derived for dry air temperature depended thermophysical properties, using respective fitted data for density as simply derived from the gas law, thermal diffusivity as derived from its definition expression and the correlations (37) and (47) for viscosity and thermal conductivity. Respective results for fixed dry air thermophysical properties corresponding to a typical average still temperature of 45 °C were also finally derived. Results are shown in Fig. 7, in which the three groups of three curves each, correspond to a temperature difference ΔT of 10, 20, and 30 °C. Solid lines correspond to results for the temperature depended saturated vapor mixture, as compared to dotted lines corresponding to temperature depended dry air and broken lines to constant average dry air properties. It can be seen that while at low average still temperatures the effect of using temperature depended dry air thermophysical properties is relatively small, at higher temperatures it leads to typically about 5% overestimation of the convective heat transfer coefficient as compared to humid air properties. However the use of constant average properties leads to significant deviations ranging typically between a 4% underestimation to a about 9% overestimation of derived results, over the entire region of operating temperatures.

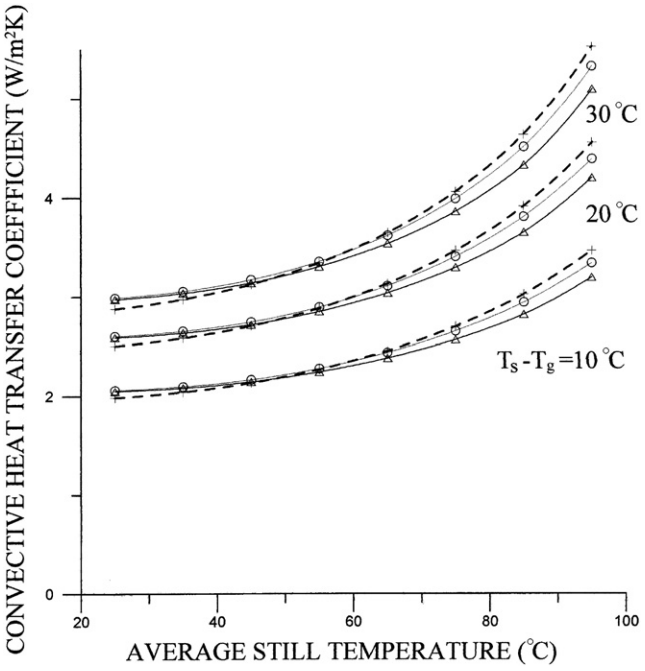

Fig. 7. The convective heat transfer coefficient plotted as a function of average still temperature between 25 and 95 °C, with a temperature difference $\Delta T = T_s - T_g = 10$, 20 and 30 °C as a parameter. Each group of the three plotted lines corresponds to derived results assuming constant average (broken lines) and temperature depended (dotted lines) properties for dry air, while solid lines correspond to results derived for thermophysical properties of a saturated mixture.

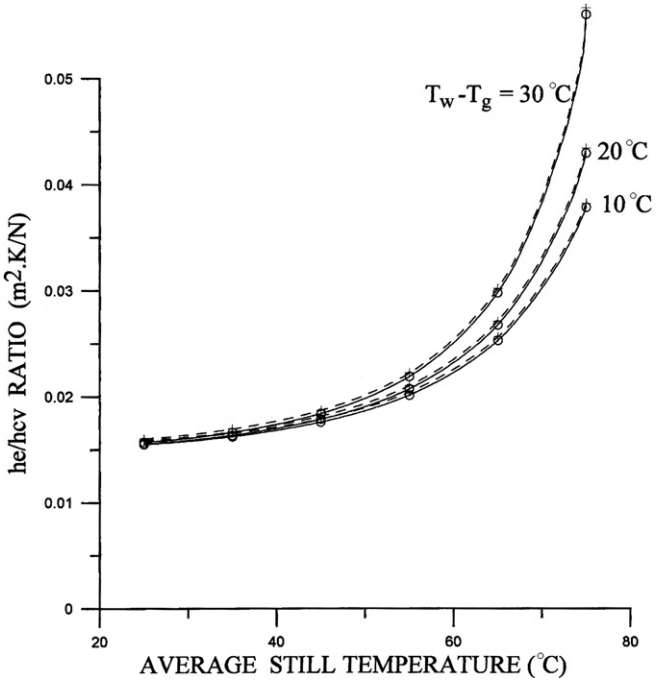

Fig. 8. The convective to evaporative heat transfer coefficient ratio plotted as a function of average still temperature with a temperature difference $\Delta T = T_s - T_g = 10$, 20 and 30 °C as a parameter. Broken lines correspond to constant average while solid lines to temperature depended data for specific heat capacity of dry air.

As derived from the expression (28), the evaporative to convective heat transfer coefficient ratio depends on the specific heat capacity of dry air. The latent heat of water vaporization in (kJ/kg) being slightly dependent on temperature, was derived by fitting of data from the standard steam tables by the following expression

$$h_{fg} = HF_0 + HF_1 t \tag{52}$$

where, $HF_0 = 2503.943143$ and $HF_1 = -2.451556893$. Assuming that R_a=0.287 kJ/kg K and $R_v = 0.4515$ kJ/kg K, the h_e/h_{cv} ratio was calculated and plotted in Fig. 8 as a function of average still temperature, with the temperature difference $\Delta T = T_w - T_g$ as a parameter. The solid lines corresponding to temperature depended and the dotted lines to the fixed average dry air specific heat capacity properties are close together showing an up to about 2% difference, something which reflects the slight dependence of the dry air specific heat capacity with temperature, as it is shown from the RH = 0 (dry air) which is the lower curve in Fig. 4. It can be seen that although for lower than about 50 °C this ratio is slightly depended on temperature with an average numerical value of about 0.017 m^2 K/N, it increases dramatically at higher temperatures owing to the effect of partial vapor pressure which decreases the product $(P_0 - P_s) \times (P_0 - P_g)$ at the denominator of (26), as the temperature increases.

The mass flow rate of distillate as calculated from the expression (30) taking into account (15), is a strong function of density, viscosity, thermal diffusivity and thermal conductivity of the saturated mixture. This quantity was calculated and plotted in Fig. 9 as a function of average still temperature with the temperature difference $T_w - T_g = 10$, 20 and 30 °C as a parameter, for fixed average and temperature depended thermophysical properties of dry air (broken and thin solid lines, respectively) and for temperature depended properties of saturated mixture (thick solid lines). Apart from the remarkable increase of mass flow rate of distillate for higher than about 50 °C temperatures and especially at higher values of $\Delta T = T_w - T_g$, it is interesting to note that although the temperature dependence of pertinent thermophysical properties of saturated mixture is significant, leading to about 70%, 26% and 20% increase of thermal diffusivity, thermal conductivity and viscosity and about 25% decrease of density as the temperature ranges between 20 and 100 °C, the overall effect on the mass flow rate is moderate. As derived from Fig. 9 although the assumption of dry air thermophysical properties, either fixed or temperature depended leads to almost identical results, it overestimates moderately the mass flow rate of distillate. This is attributed to the fact that although the quantity $(\rho_m/\mu_m \times \alpha_m)$ decreases dramatically and becomes a small fraction of about 37% of its initial value as the temperature increases between 20 and 100 °C, this effect is compensated by the influence of exponent 1/3 and the corresponding increase of the multiplier k_{av} with temperature in the expression (15), which leads to about 6.5% overestimation of derived results for average still temperature of 75 °C and up to about 10% for the maximum temperature of 100 °C.

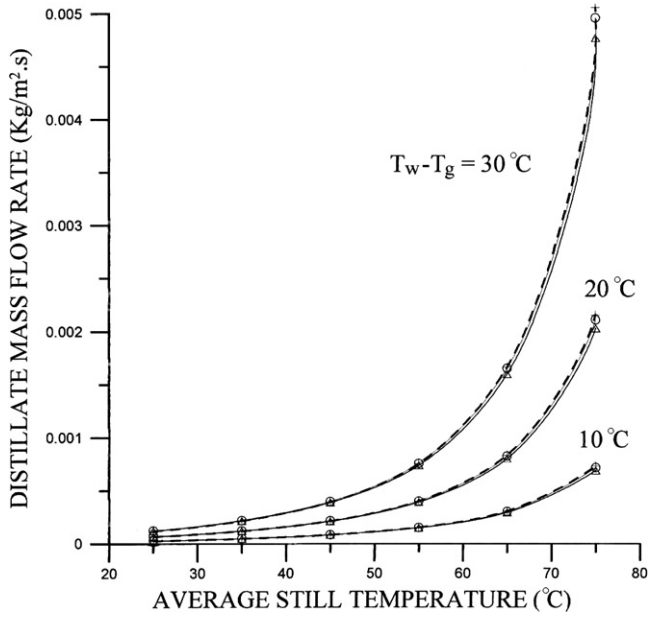

Fig. 9. The distillate mass flow rate plotted as a function of the average still temperature with a temperature difference $\Delta T = T_s - T_g = 10$, 20 and 30 °C as a parameter. Broken lines correspond to constant average, while thin solid lines to temperature depended thermophysical properties of dry air as compared to derived results using thermophysical properties for a saturated mixture (solid lines).

5. Conclusions

In the present investigation an analysis was developed aiming to underline the significance of employing the appropriate thermophysical properties on the theoretical prediction of the most significant parameters influencing the heat and mass transfer processes in solar stills. An analysis was also presented aiming at the description of simplified procedures from the literature for the evaluation of the main thermophysical properties of binary mixtures of water vapor and dry air. Based on this analysis, the calculation of the full range of water vapour and dry air mixture properties was carried out and the results were fitted at saturation conditions through simple polynominal expressions suitable for computerised calculations. The derived results were employed to investigate the effect of using proper thermophysical data corresponding to a saturated mixture, on the prediction accuracy of the most significant heat and mass transfer parameters during the operation of the solar stills. It was found that although the use of dry air properties leads to a significant overestimation of the convective heat transfer coefficient, especially at the high temperature range of operation, the deviations associated to the mass flow rates are moderate, leading to up to about 10% maximum errors comparably to saturated mixture properties.

References

Aggrawal, S., Tiwari, G.N., 1998. Convective mass transfer in double-condensing chamber and a convective solar still. Desalination 115, 181–188.

Ahmed, S.T., 1988. Study of single-effect solar still with an internal condenser. Solar & Wind Technology 5 (6), 637–643.

Alduchov, O.A., Escridge, R.E., 1997. Improved Magnus Form Approximation of Saturation Vapor Pressure, Technical Report DOE/ER/61011-T6, November 1997, National Climatic Data Center, National Oceanic and Atmospheric Administration, Asheville, NC 28801.

Al Mahdi, N., 1992. Performance prediction of a multi-basin solar still. Energy 17 (1), 87–93.

Clark, J.A., 1990. The steady-state performance of a solar still. Solar Energy 44 (1), 43–49.

Cooper, P.I., 1969. Digital simulation of transient solar still processes. Solar Energy 12, 313–331.

Coulson, J.M., Richardson, J.F., 1961. In: Chemical Engineering, vol. 1. Pergamon Press, Oxford, London, N.Y.

Duncle, R.V., 1961. Solar water distillation: the roof typestill and a multiple effect diffusion still. ASME Proc. Int. Heat Transfer Conf. Part V. In: Int. Develop. Heat Transfer. University of Colorado, Boulder Colo.

Fath, H.E.S., Elsherbiny, S.M., 1992. Effect of adding a passive condenser on solar still performance. Int. J. Solar Energy 11, 73–89.

Giacomo, P., 1982. Equation for the determination of the density of the moist air (1981). Metrologia 18, 33–40.

Haddat, O.M., Al-Nimr, M.A., Maqableh, A., 2000. Enhanced solar still performance using a radiative cooling system. Ren. Energy 21, 459–469.

Hollands, K.G.T., Raithby, G.T., Konicek, L., 1975. Correlation equations for free convection heat transfer in horizontal layers of air and water. Int. J. Heat Mass Transfer 18, 879–884.

Irvine Jr., T.F., 1998. Thermophysical properties. In: Rohsenow, W.M., Hartnett, J.P., Cho, Y.I. (Eds.), Handbook of Heat Transfer, Chapter 2, third ed. McGraw-Hill, N.Y. San Fransisco.

Irvine, T.F., Liley, P., 1984. Steam and Gas Tables with Computer Equations. Academic Press, San Diego.

Krischer, O., Kast, W., 1978. Trocknungstechnik-Die wissenschaftlichen Grundlagen der Trocknunngstechnik, third ed.. In: vol. 1 Springer, Berlin, Heidelberg.

Kumar, S., Tiwari, G.N., 1996. Estimation of convective mass transfer in solar distillation systems. Solar Energy 57 (6), 459–464.

Lof, G.O.G., 1980. Solar distillation. In: Springler, K.S., Laird, H.D.K. (Eds.), Principles of Desalination, chapter 11 Part B, second ed. Academic Press, N.Y. London, San Francisco, pp. 679–723.

Malik, M.A.S., Tiwari, G.N., Kumar, A., Sodha, M.S., 1982. Solar Distillation. Pergamon Press, Oxford, N.Y.

McAdams, W.H., 1981. Heat Transmission, third ed. McGraw-Hill, N.Y., 16th printing.

Melling, A., Noppenberger, S., Still, M., Venzke, H., 1997. Interpolation Correlations for Fluid Properties of Humid Air in the Temperature Range 100 °C to 200 °C. J. Phys. Chem. Ref. Data 26 (4), 1111–1123.

Rahim, N.A., Taqi, E., 1992. Comparison of free and forced condensing systems in solar desalination units. Ren. Energy 2 (4/5), 405–410.

Tiwari, G.N., Singh, A.K., Saxena, P., Rai, S.N., 1993. The performance of multi-effect active distillation system. Int. J. Solar Energy 13, 277–287.

Tiwari, G.N., Minoha, A., Sharma, P.B., Khan, M.E., 1997. Simulation of convective mass transfer in a solar distillation process. Energy Conv. & Management 38, 761–770.

Toulukian, Y.S., Powell, R.W., Ho, C.Y., Clemend, P.G., 1970. Thermophysical Properties of Matter, vol. 1. N.Y.

Toyama, S., Aragaki, T., Salah, H.M., Murase, K., Sando, M., 1987. Simulation of a multieffect solar still and the static characteristics. J. Chem. Eng. Jpn. 20 (5), 473–478.

Van Wilen, G.J., Sonntag, R.E., 1973. Fundamentals of Classical Thermodynamics. Wiley, N.Y.

Wong, G.S.K., Embleton, T.F.W., 1984. Variation of specific heats and of specific heat ratio in air with humidity. J. Acoust. Soc. Am. 76 (2), 555–559.

Zuckerwar, A.J., Meredith, R.W., 1985. Low-frequency absorption of sound in air. J. Acoust. Soc. Am. 78 (3), 946–955.